ELSEVIER

Edge-enhanced spatiotemporal constrained reconstruction of undersampled dynamic contrast-enhanced radial MRI

Srikant Kamesh Iyer [a,b,c], Tolga Tasdizen [a,b], Edward V.R. DiBella [c,d,*]

[a]Electrical and Computer Engineering Department, University of Utah, Salt Lake City, UT, USA
[b]SCI Institute, School of Computing, University of Utah, Salt Lake City, UT, USA
[c]UCAIR, Department of Radiology, University of Utah, Salt Lake City, UT, USA
[d]Department of Bioengineering, University of Utah, Salt Lake City, UT, USA

Abstract

Dynamic contrast-enhanced magnetic resonance imaging (MRI) is a technique used to study and track contrast kinetics in an area of interest in the body over time. Reconstruction of images with high contrast and sharp edges from undersampled data is a challenge. While good results have been reported using a radial acquisition and a spatiotemporal constrained reconstruction (STCR) method, we propose improvements from using spatially adaptive weighting and an additional edge-based constraint. The new method uses intensity gradients from a sliding window reference image to improve the sharpness of edges in the reconstructed image. The method was tested on eight radial cardiac perfusion data sets with 24 rays and compared to the STCR method. The reconstructions showed that the new method, termed edge-enhanced spatiotemporal constrained reconstruction, was able to reconstruct images with sharper edges, and there were a 36%±13.7% increase in contrast-to-noise ratio and a 24%±11% increase in contrast near the edges when compared to STCR. The novelty of this paper is the combination of spatially adaptive weighting for spatial total variation (TV) constraint along with a gradient matching term to improve the sharpness of edges. The edge map from a reference image allows the reconstruction to trade-off between TV and edge enhancement, depending on the spatially varying weighting provided by the edge map.
© 2012 Elsevier Inc. All rights reserved.

Keywords: MRI; Reconstruction; Edge enhanced; Compressed sensing; Regularization; Cardiac perfusion

1. Introduction

In dynamic contrast-enhanced magnetic resonance imaging (DCE-MRI), a gadolinium (Gd)-based contrast agent is injected into the patient, and the T1 shortening effect of Gd makes regions that receive the contrast appear bright in the acquired T1-weighted images. To follow the dynamics of the contrast agent, high temporal and high spatial resolution is required. The MRI scanner requires a relatively large amount of time to acquire full data in k-space. Hence, simultaneous achievement of both high spatial resolution and high temporal resolution is challenging. When less data are acquired in k-space, a linear reconstruction scheme causes artifacts to appear in the image. The sampling pattern and its point spread function [1] determine the type of artifacts seen.

In the case of radial acquisition, these artifacts appear as streaks across the image.

One major application of DCE-MRI is myocardial perfusion imaging. DCE cardiac perfusion imaging is an important clinical tool used to assess blood flow to the myocardium in order to detect coronary artery disease. Radial acquisition has been used in DCE cardiac perfusion imaging in part because radial acquisitions are relatively more robust to motion when compared to Cartesian acquisition. The reconstruction algorithm used to reconstruct the images from the undersampled k-space data must be able to reconstruct images with good contrast and sharp edges and must also be robust to some motion in the acquired data.

There have been many methods proposed to handle the problem of incomplete k-space data. Techniques like keyhole [2,3], reduced-encoding imaging with generalized-series reconstruction (RIGR) [4,5] and sliding window [6] have been used for reconstructing contrast-enhanced images

and are relatively simple to implement. Most streaking artifacts in the image can be removed by these techniques, but images with high spatial and temporal resolution are often not achievable for high undersampling factors. Smaller structures and edges in the image often become blurred, and in the presence of respiratory motion, techniques like sliding window and keyhole perform poorly. This prevents their widespread use in cardiac perfusion imaging.

Cardiac images have high spatiotemporal correlations. Techniques like k-t Broad-use Linear Acquisition Speed-up Technique (BLAST) and k-t SENSitivity Encoding (SENSE) [7] exploit the spatiotemporal correlation by using dynamic training data. This helps in achieving high acceleration factors and also images with high resolution. But if there are inconsistencies between the training data and the reconstructed images, the method performs poorly. This reportedly makes k-t SENSE less robust to motion [8]. To overcome these limitations, the spatiotemporal domain-based unaliasing employing sensitivity encoding and adaptive regularization [9] algorithm used RIGR for its initial estimates. This reduces the problems associated with using a temporal average that is used in k-t BLAST and k-t SENSE and makes the method more robust to motion.

The idea of compressed sensing (CS) [1] aims to leverage sparsity constraints to reconstruct artifact-free images from relatively few k-space samples. k-t FOCal Underdetermined System Solver (FOCUSS) [10,11] and k-t SPARSE [12] are CS-based schemes that use the Fourier transform along the temporal domain as the sparsifying transform. These methods have been shown to be robust to motion [8]. CS-based methods can also be combined with parallel imaging techniques [8,13,14] to accelerate parallel imaging further.

Another way of exploiting the temporal correlations in DCE cardiac perfusion images in a CS framework is the use of temporal gradients as sparsifying constraints. Temporally constrained reconstruction [15,16] and, subsequently, a spatiotemporal constrained reconstruction (STCR) [17] have been shown to give good quality reconstructions of undersampled cardiac perfusion images with some respiratory motion using radial data with 24 rays. Here we propose to extend STCR in two ways. The first is to make the weight on the spatial constraint spatially varying. Such a spatially varying constraint was presented in Refs. [18–20]. In Ref. [18], a local noise measure was used to determine the spatial total variation (TV) constraint weight, with greater noise using higher weights. In Refs. [19,20], the scale of the objects in the image and the noise in the image were used to determine the weights of spatial TV constraint. In our method, the spatially varying weight is determined by edge strength. The second extension proposed here is to improve the sharpness of edges by adding an edge matching function based on a reference image. The new method is thus termed edge-enhanced spatiotemporal constrained reconstruction (EESTCR) [21].

2. Theory and method

2.1. Shortcomings of TV constraints

In Refs. [19,22], it was shown that TV denoising could lead to loss of contrast. In order to overcome the problem of loss of contrast due to TV, a spatially varying weight for TV was proposed by Strong and Chan in Ref. [20]. It was shown that a spatially varying weight for TV performs better at preserving contrast and also smaller features in the image. Two methods to make the weight spatially varying, namely, by using information about the size of different objects in the image, or by using information about noise in the image, were also developed. When reconstructing cardiac images, weight for TV should be large at uniform regions in the image to remove streaking artifacts and noise, while the weight should be small at edges to avoid smoothing and loss of contrast. Our method is motivated with this realization and proposes an automatic way to handle spatially varying weights by making use of information from a reference image.

2.2. EESTCR formulation

Aliasing artifacts occur in the image when Cartesian k-space is undersampled. When radial sampling is used, these artifacts appear as streaks in the image. However, any prior knowledge about the fully sampled image can be incorporated as constraints in a regularization framework to reduce or remove these artifacts. In EESTCR, the images are reconstructed by minimizing

$$C = \|Em - d\|_2^2 + \alpha_1 \sum_{i=1}^{N} \|\nabla_t m_i\|_1 \qquad (1)$$
$$+ \alpha_2 \sum_{j=1}^{T} \|(1 - \omega_j) \nabla m_j\|_1$$
$$+ \alpha_3 \sum_{j=1}^{T} \|\omega_j^{1/2}(\nabla m_j - \nabla I_j^r)\|_2^2,$$

Where m represents the estimated complex image data and E is a matrix that models the physical imaging process. For MRI, E includes the k-space trajectory and also the Fourier transform operator. The fidelity term is given by $\|Em - d\|_2^2$, where $\|.\|_2$ represents the L_2 norm and d is the acquired sparse k-space data. The temporal regularization term is a TV in time penalty given by $\sum_{i=1}^{N} \|\nabla_t m_i\|_1$, where ∇_t is the temporal gradient operator, N is the total number of pixels in each time frame and m_i represents the time curve of pixel i. The spatial regularization term is a spatial TV [23,24] penalty given by $\sum_{j=1}^{T} \|\nabla m_j\|_1$, where $\|.\|_1$ represents the L_1 norm, T is the total number of time frames and ∇ represents the spatial gradient operator. The spatial TV constraint was implemented as shown in Ref. [16]. To improve the sharpness of the edges, we propose to add an edge constraint

given by $\sum_{j=1}^{T} ||\omega_j^{1/2}(\nabla m_j - \nabla I_j^r)||_2^2$, where I^r is the reference image and ω is a spatially varying weight defined as $\omega=1-\exp(-|(\nabla I^r)^2|/\lambda^2)$, in which λ is a constant. α_1, α_2 and α_3 are weights that control the amount of spatial TV regularization, temporal regularization and the gradient matching term, respectively. The reference image for each time frame is formed by combining three previous frames with the current time frame in a sliding window fashion. This allows each time frame to have its own reference image that follows the dynamics and motion of the acquired data.

The function $\omega(x,y,t)$ is used to form a spatially varying edge map of the strength of the edges in the reference image. It is assumed that the reference image does not suffer from artifacts due to incomplete k-space acquisition. The term $(1-\omega)$ is used to control the influence of the TV minimization at areas where the gradient of the reference image is large. At such points, the value of ω is close to 1, and hence, $(1-\omega)$ is almost zero. These low values of $(1-\omega)$ prevent the influence of TV minimization at sharp edges where only the edge matching function takes effect. This adaptive weighting leads to improvement of the sharpness of the edges by the edge constraint, and at the same time, the streaking and noise are removed by the spatial and temporal regularization terms.

An iterative gradient descent scheme with finite forward differences [25] was used to minimize the cost function. The dynamic series of images was updated at every iteration according to the following equation:

$$m_{n+1} = m_n - \eta C'(m_n); n = 1, 2, ... \qquad (2)$$

Here n is the iteration number, η is the step size and C' is the Euler–Lagrange derivative of the cost functional with respect to m. The Euler–Lagrange derivative of the edge matching function is given by $\alpha_3\omega(\nabla^2 m - \nabla^2 I^r)$.

2.3. Data acquisition

The radial perfusion data were obtained using a Siemens Trio 3-T scanner with a phased array cardiac coil. A saturation recovery turbo flash sequence with repetition time/echo time ~2.5/1.4 ms, 12° flip angle and 8-mm slice thickness was used. The radial data had 24 rays in each time frame. A different start angle offset equal to an integer multiple of $(180/96)°$ was used, and this was repeated every four frames so that a combination of four frames gave 96 unique equiangular rays. The method was tested on eight radial data sets acquired from six patients (four males and two females). Six data sets were acquired at rest, and two were acquired at stress. The contrast agent Gd-BOPTA, 0.03–0.04 mmol/kg, 5 cc/s, was used for rest and adenosine stress perfusion. The data were acquired with shallow breathing. The data were obtained using 9 to 15 receive coils of which 3–5 combined "coils" were reconstructed separately and 5 to 10 slices were acquired per study.

2.4. Reconstruction

First, the k-space data for each study were scaled to have the same range of intensities. The radial k-space samples were then interpolated onto a Cartesian grid for faster iterations as discussed in Ref. [16]. A reference frame for each reconstructed time frame was then created by combining the inverse Fourier transform (IFT) of the current time frame with the IFT of three frames before it in a sliding window fashion.

In order to determine the reconstruction parameters for EESTCR, a training data set was used. One of the eight patient data sets was chosen as the training data set, and it consisted of 8 slices and 53 time frames. To calculate the weight α_1, the L-curve technique was used. The weights α_2 and α_3 were set to zero. The elbow point in the L-curve corresponds to the best balance between the fidelity norm and temporal norm. We found that this elbow point was close to $\alpha_1=0.05$ for each of the eight slices. An example is shown in Fig. (1). The weights α_2 and α_3 were then chosen empirically for the test data set. The regularization weights were chosen as $\alpha_1=0.05$, $\alpha_2=0.005$ and $\alpha_3=0.1$. To choose the step size and the number of iterations for the reconstruction, the cost function was plotted against the number of iterations, and a combination of step size and number of iterations that led to a stable minimum was determined for the test data set. The step size for the gradient descent minimization was fixed at 0.05, and 150 iterations were performed to minimize the cost function C in Eq. (1). For the edge function ω, the value of λ was chosen as $\lambda=0.045$. The λ value that appeared to give the sharpest edges in the edge map ω was used.
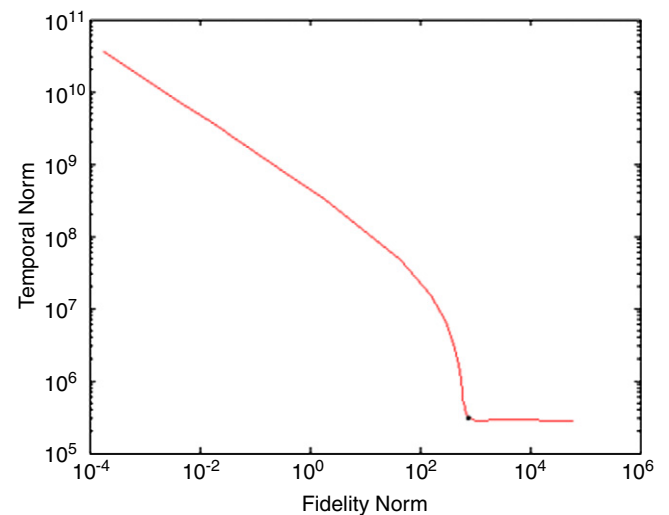

Fig. 1. An L-curve for one of the data sets used is shown. The elbow point in the log–log plot of the fidelity norm versus the temporal norm is $\alpha_1=0.05$, shown by a dark point. Though the L-curve for only one slice is shown here, the elbow point for all of the slices was in a similar position. The α_1 values were continuously varied between 10^{-6} and 5.

Reconstructions were performed on data from each coil independently, and the images were combined using square root of sum of squares. The coils used to create the final images were chosen by visual inspection. This was done to avoid coils that produced heavy streaking artifacts.

2.5. Robustness of the method to small changes in the weights

To test the robustness of the method to small changes in the weights, the weights α_1, α_2 and α_3 were changed by ±20%, ±20% and ±50%, respectively, in different combinations of the three weights. Comparisons were made with images reconstructed using $\alpha_1=0.05$, $\alpha_2=0.005$ and $\alpha_3=0.1$.

2.6. Comparison metrics

To compare the images reconstructed using EESTCR and STCR, we used a difference image. Plots of values in a line across the myocardium were also used to study the differences. The same line was plotted over time for both the methods, and a percentage difference between the two reconstruction methods was calculated. To study the robustness of EESTCR to motion, the method was applied to another set of three more patient data sets with large respiratory motion. The reconstructed images were compared with those of STCR for artifacts and false edges.

Contrast-to-noise ratio (CNR) and contrast were also calculated. Here CNR is given by the ratio $\frac{\left(MI_{Blood} - MI_{Myo}\right)}{\sigma_{Bkg}}$, where MI_{Blood} is the mean intensity of a small region in the left ventricle (LV) blood pool, MI_{Myo} is the mean intensity of a small region in the myocardium and σ_{Bkg} is the standard deviation of a region in the background. Contrast is computed as $\frac{\left(MI_{Blood} - MI_{Myo}\right)}{\left(MI_{Blood} + MI_{Myo}\right)}$. CNR and contrast were calculated from a single time frame when the mean intensity in the LV blood pool was maximum and the regions were chosen close to the edge of the septal wall Fig. 2(A).
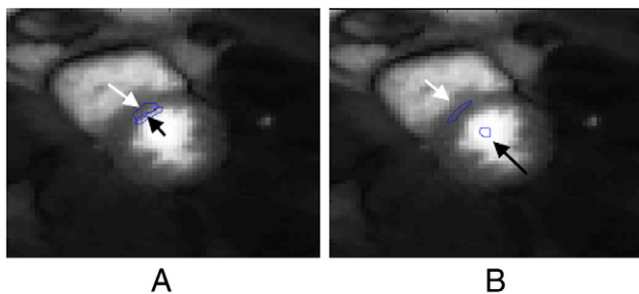

Fig. 2. Comparison of CNR and contrast for two choices of ROI. The regions are chosen (A) close to the edge in the myocardium and LV blood pool and (B) away from the edge. For the ROI shown in (A), CNR=88.12 and contrast=0.25 for EESTCR, and CNR=58.50 and contrast=0.18 for STCR. There are a 50.6% increase in CNR and a 39% increase in contrast. For the ROI shown in (B), no significant change in CNR and contrast was seen. CNR=250.2 and contrast=0.54 using EESTCR, and CNR=252 and contrast=0.53 using STCR.

3. Results

In general, the series of images reconstructed using EESTCR have better contrast and sharper edges than STCR results. The images in Figs. 3 and 4 show the improvement of edges in the LV and in the right ventricle (RV). The difference image shows that, in EESTCR, smoothing of edges is avoided and sharper edges are reconstructed. Also, the difference between the myocardium and blood pool is clearer in the EESTCR images when compared to STCR.

When trying to detect regions in the myocardium that have a perfusion defect, good contrast improves the ease with which such regions can be detected. This change in contrast in the region with less flow can be subtle in the reconstructed images. The images in Fig. 3 show that in the ischemic region in the myocardium [shown by the white arrow in Fig. 3(B) and (C)], the decrease in contrast in the myocardium is more visible in the image reconstructed using EESTCR. In the plot of the line in myocardium over time in Fig. 3(F), the difference is greatest at the edges of the LV myocardium. The spatial location of the line is shown in Fig. 3(A). The change in the line intensities across the myocardium plotted in Fig. 3(E) also shows that the valleys are lower and peaks are higher.

Sharper edges with EESTCR are shown for two time frames in Fig. 4. The difference between the myocardium and blood pool is more visible in images reconstructed using EESTCR. Also, finer structures like papillary muscles and the myocardium are better visualized in EESTCR. In STCR, finer structures can be mistaken for noise in the image, and these structures in the reconstructed image can be smoothed or removed. In EESTCR, by using a reference image to reduce the spatial TV weight at locations in the reconstructed image which are likely to have edges, this smoothing effect of TV is avoided.

The direction in which the intensities in the images reconstructed using EESTCR changed when compared to STCR is in a direction such as to increase the contrast in the image as opposed to STCR which will be in a direction such as to decrease the contrast in the image. In Fig. 5, we see that when gadolinium is present in the LV or RV, a 25% difference in the intensity between STCR and EESTCR was seen in the myocardium and the edges in LV and RV. The presence of gadolinium allowed improved detection of edges, and the edge map could be used by the gradient matching term to make the edges sharper. This difference was seen in a series of 10–15 time frames as shown in Fig. 5(D).

3.1. Robustness of the reconstruction to small changes in weights

We found that the method was robust to small changes in weights. A mean squared difference-based comparison of images reconstructed using the new set of weights that
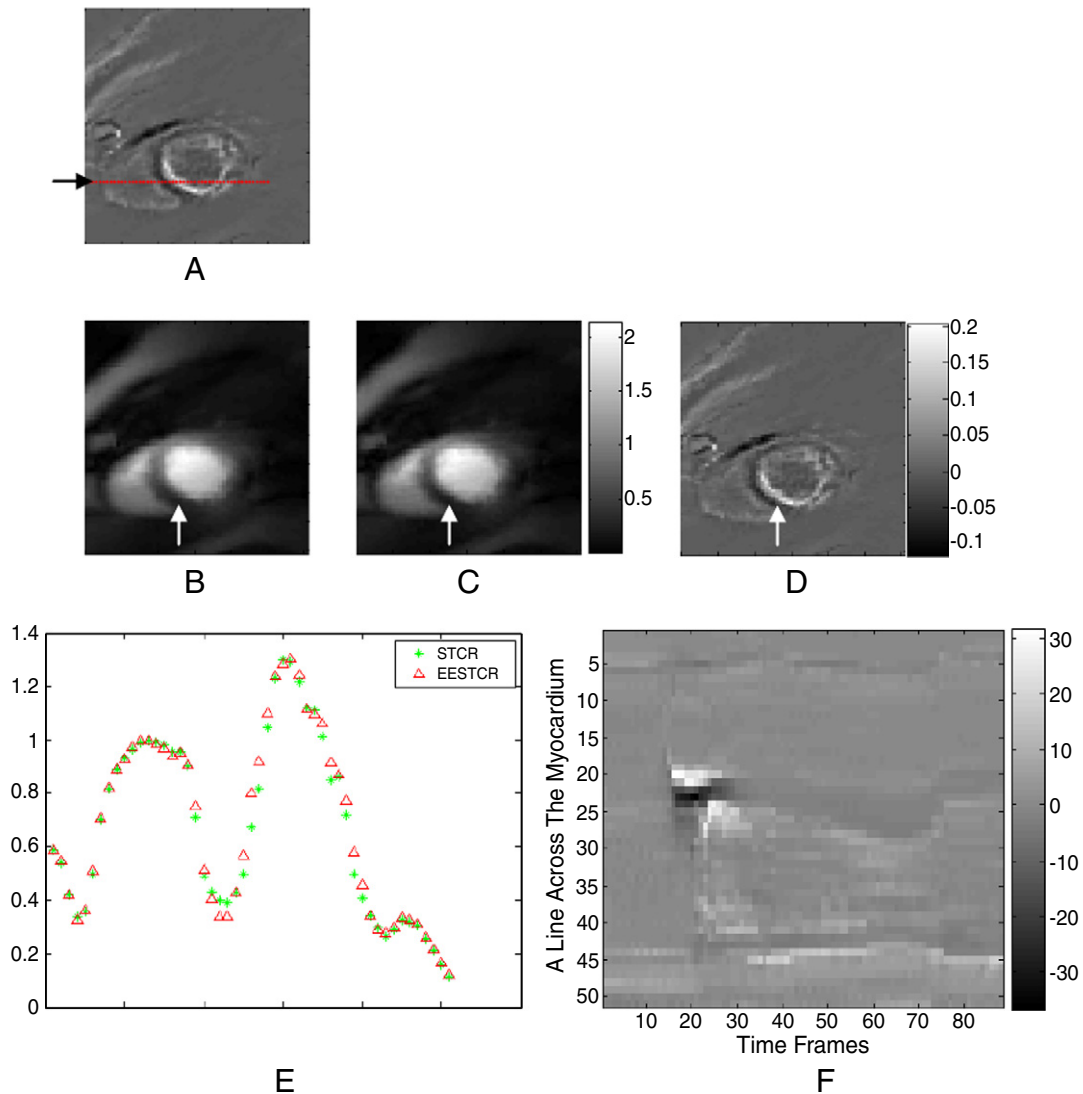
Fig. 3. The effect of using EESTCR when compared with STCR in a patient with ischemia. The images were reconstructed from radial data containing 24 rays. (A) Dotted line showing the spatial location of the plots. (B) Reconstructions using STCR, (C) reconstructions using EESTCR and (D) the difference image formed by taking the difference between EESTCR reconstruction in 1(C) and STCR reconstruction in 1(B). (E) Comparison of cross-sectional plot of a horizontal line across the myocardium as shown in 3(A). (F) A plot of the line across the myocardium in the difference image over time. The difference is shown in percentage scale.

had small perturbations and the standard set of weights showed that the differences were very small, usually in the order of 10^{-5} to 10^{-6}. An example is shown in Fig. 6. The maximum mean squared error seen in this data set was 7.6×10^{-6}.

3.2. Robustness to motion

There was respiratory motion present in the images shown in Figs. 3 and 4. Even in the presence of some motion, EESTCR was able to reconstruct images with sharper edges, showing that the method is robust to some motion. We found that, in some data sets, a good edge map could not be extracted because of a poor reference image. In such data sets, only slight or no improvement was seen

in the sharpness of edges. However, a poor reference frame did not degrade the image quality, and the reconstructed image quality was very similar to STCR. The images in Fig. 7 show examples of a good edge map [Fig. 7(A)] and a poor edge map [Fig. 7(D)].

The performance of EESTCR on data sets with large motion and data sets with minimal motion is shown in Fig. 7. The edge map shown in Fig. 7(D) is blurred due to motion in the vertical direction. This causes the edges to appear broader in the edge map. Because the edges are blurred, the edge map detects edges at locations that may not correspond to edges in the reconstructed image. These blurred edges are usually less strong when compared to sharp edges, and hence, the weight on the edge matching function is no longer large. The method was used on three
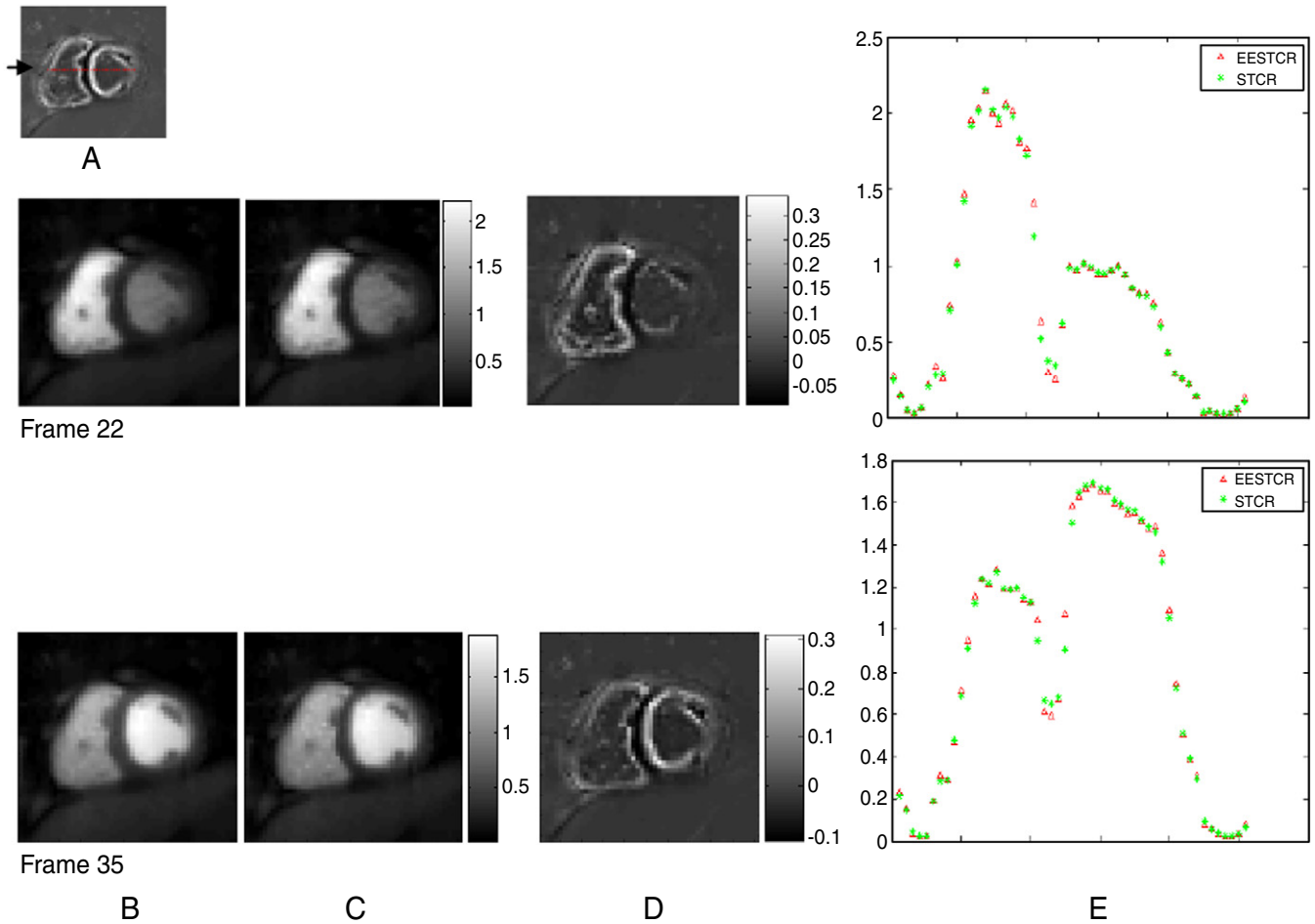
Fig. 4. Two time frames when Gd is present in the RV and LV, respectively. (A) Dotted line showing the location of the cross-sectional plot. (B) Images reconstructed using STCR, (C) images reconstructed using EESTCR and (D) the image difference between EESTCR (C) and STCR (B). (E) The cross-sectional plot of EESTCR and STCR across a horizontal line in the myocardium as shown by a dotted line in the image 4(A). The intensities at the lower edges have decreased, the intensities at the upper edge have increased, and better contrast is visible in EESTCR reconstructions.

data sets with large respiratory motion, and comparisons with STCR showed that no edge artifacts were added due to EESTCR. The images reconstructed using EESTCR matched those using STCR in image quality.

We found that if coils that had heavy streaking artifacts, such as from bright fat signal near the coil, were used for reconstruction, these streaking artifacts were added as false edges in the reconstructed image. This is because the weight added due to the edge map is no longer small and the presence of the artifacts in the acquired data at such locations would make the gradient matching term enhance the streaks. This problem can be mitigated by not choosing coils that have heavy streaking artifacts in them. The coils for the reconstructions were chosen by visual inspection.

3.3. Effect of EESTCR on segmentation

Manual registration and segmentation are often performed on the series of reconstructed images. This is done to extract time curves and flow reserves from the dynamic series of images. Contours have to be drawn around the myocardium to aid in the process of registration and segmentation. The presence of partial volume effect hinders this process. Also, signal from the blood pool should not be included with the myocardium during segmentation. The partial volume effect near the myocardium–blood pool interface is less in EESTCR when compared with STCR. This made the process of drawing contours easier. The contours with EESTCR images were often more conservative when compared with STCR, and the signal from the blood pool could be carefully avoided in the myocardium.

An example of the manual contours is shown in Fig. 8. The contours were first drawn on STCR [Fig. 8(A)] and overlaid on EESTCR [Fig. 8(B)]. The contours do not match the edges well, and signal from the blood pool in the LV and RV gets included with the myocardium in EESTCR. These regions are shown by the two black arrows in Fig. 8. A more conservative or narrow contour would have been drawn on
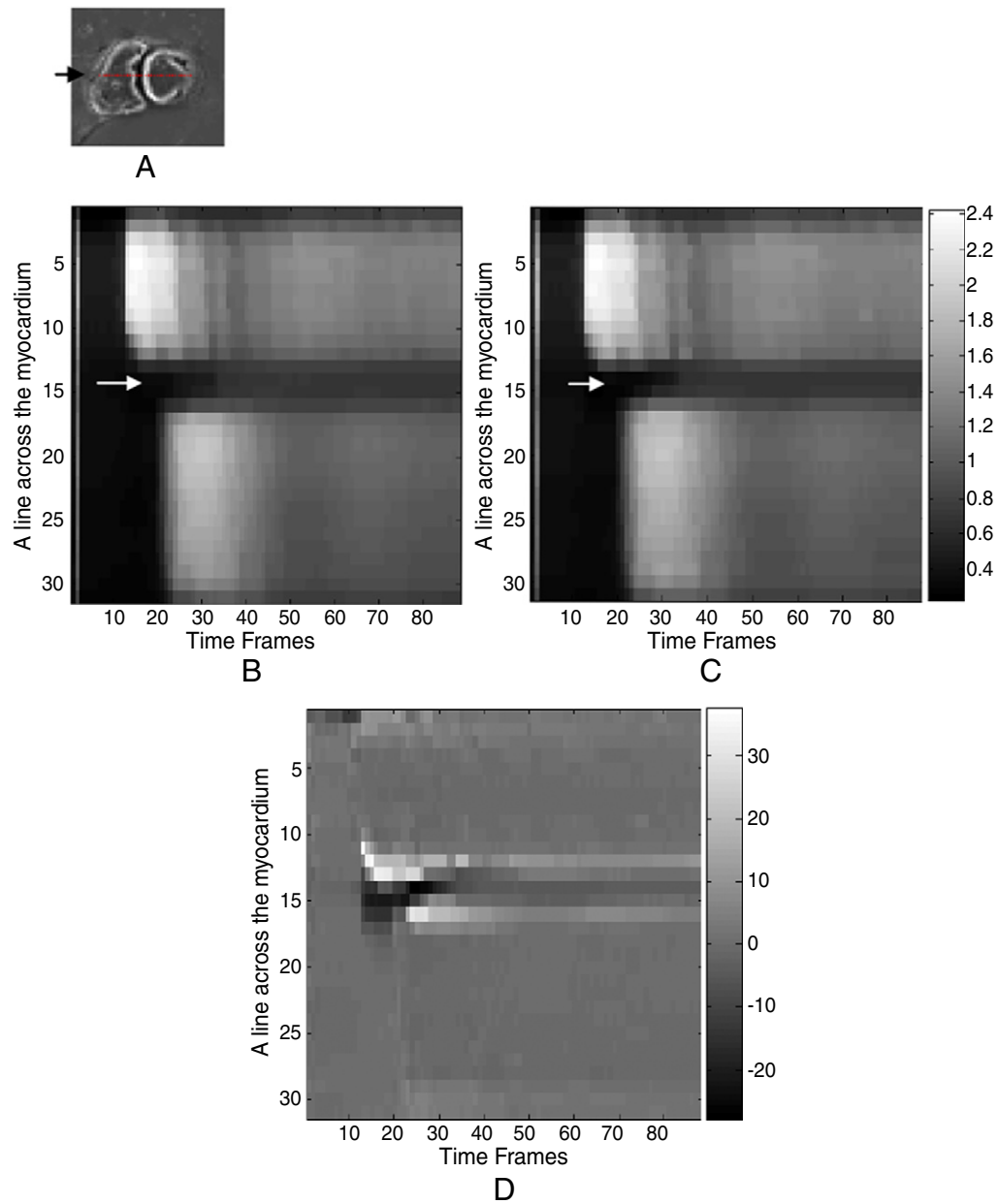
Fig. 5. The plot of a line across the myocardium over time. (A) The spatial location of the line. The plot of the line for image reconstructed using (B) STCR and (C) EESTCR is shown. (D) The percentage difference between (A) STCR and (B) EESTCR.

EESTCR image to avoid the blood pool signal from being included with the myocardium.

3.4. CNR and contrast

To calculate the CNR and contrast of images reconstructed using STCR and EESTCR, regions of interest were selected close to the edge of the myocardium and the LV blood pool, as shown in Fig. 2(A). There was on average a 36%±13.7% increase in the CNR and a 24%±11% increase in the contrast in images reconstructed using EESTCR when compared with STCR in five data sets. The standard deviations of the background for EESTCR and STCR

reconstructed images were similar. When the standard deviation of a small region in the center of the blood pool was used instead of the standard deviation of the background, a similar percentage increase in CNR was seen.

For the example shown in Fig. 2(A), the CNR and contrast computed using EESTCR were CNR=88.12 and contrast=0.25. For STCR, CNR=58.5 and contrast=0.18. There were a 50.6% increase in CNR and a 39% increase in CR in this example. If the regions of interest were chosen well within the myocardium and blood pool, away from the edges [as shown in Fig. 2(B)], no significant change in CNR and contrast was seen. For the example shown in Fig. 2(B), CNR=250.2 and contrast=0.54 for EESTCR, and CNR=252
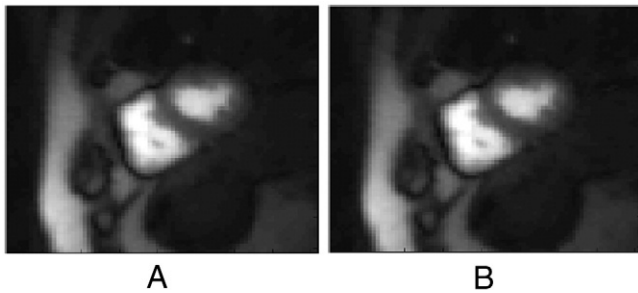
Fig. 6. Robustness of the reconstruction technique to small changes in the weights is shown. (A) Single coil image reconstructed using standard set of weights chosen: $\alpha_1=0.05$, $\alpha_2=0.005$ and $\alpha_3=0.1$. (B) Image reconstructed using $\alpha_1=0.06$, $\alpha_2=0.004$ and $\alpha_3=0.05$. The mean squared difference between (A) and (B) is 7.6×10^{-6}. This shows that the reconstruction algorithm is robust to small changes in the weights.

reference image that is generated from the undersampled data are used for this purpose. Unlike uniformly weighted TV, which can cause loss of contrast and smoothing of fine features in the image, in EESTCR, the spatially varying edge map makes the weight for TV spatially varying, and the smoothing effect of TV is avoided. The gradient matching term also enhances the edges in the reconstructed image by using an L_2 norm penalty with respect to the gradients of a reference image. The result of this edge enhancement is seen in the difference image and the cross sectional plots in Figs. 3 and 4. These show that EESTCR is better at handling trade-offs between smoothness of uniform regions and sharpness of edges. In data sets with large respiratory motion where only poor reference images with blurred edge maps could be extracted, the reconstructed image quality was comparable with STCR, and no false edge artifacts were added to the reconstructed image. This is because blurred edges usually tend to be less strong when compared with sharper edges. The presence of the temporal constraint at every pixel in the image also helps avoid these artifacts.

The temporal constraint is used to exploit the correlations in time of every pixel. As discussed in Ref. [16], the effect of the temporal constraint on the reconstructed image is more significant when compared to the spatial TV constraint. As a part of future work, spatially varying weights for the temporal constraint could be used so that different locations in the curve would be weighted differently. Any other information that can be extracted from the reference image, like the distribution of intensities, could also be used as a constraint in the reconstruction.

and contrast=0.53 for STCR. This shows that there is better contrast in EESTCR reconstructed images near the edges when compared to STCR. High contrast near the LV blood pool–myocardium boundary can help in the accurate detection of subendocardial ischemia.

4. Discussion

A new gradient matching term-based image reconstruction algorithm is presented. EESTCR is a data-driven approach to make the weight on the TV regularization spatially varying. Spatial gradients of a sliding window
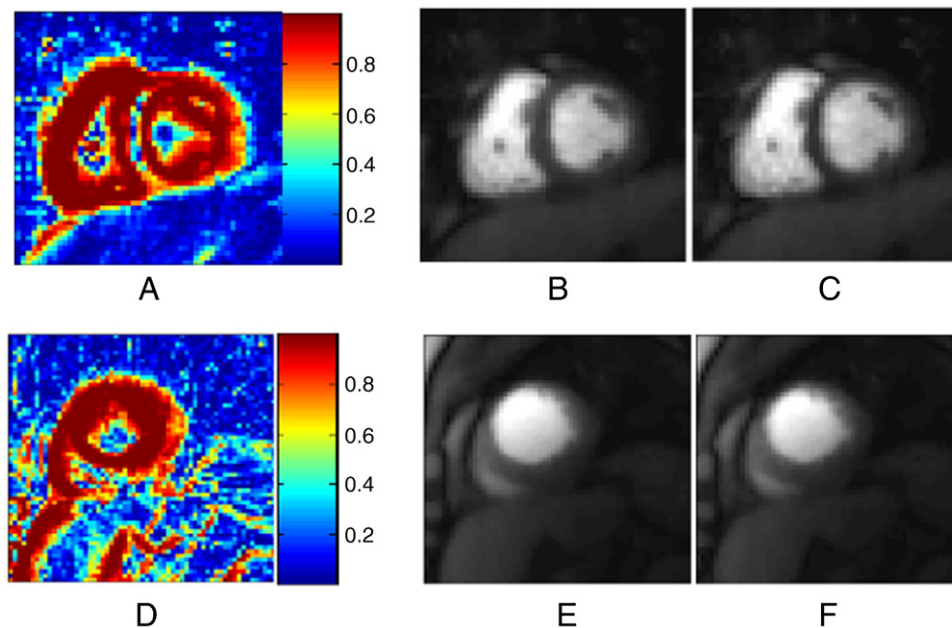

Fig. 7. The effect of reference images with different image qualities and their corresponding effect on the reconstructed image. (A) A good edge map. (B and C) The images reconstructed using STCR and EESTCR, respectively. The image reconstructed using EESTCR (C) has sharper edges as compared to STCR (B). The comparison is further shown in Figs. 4 and 5. (D–F) The effect of using a poor reference image, whose edges are blurred due to motion, as seen in 6(D). The reconstructions using EESTCR (F) are comparable with STCR (E). No false edges or artifacts have been added due to the blurred reference image.
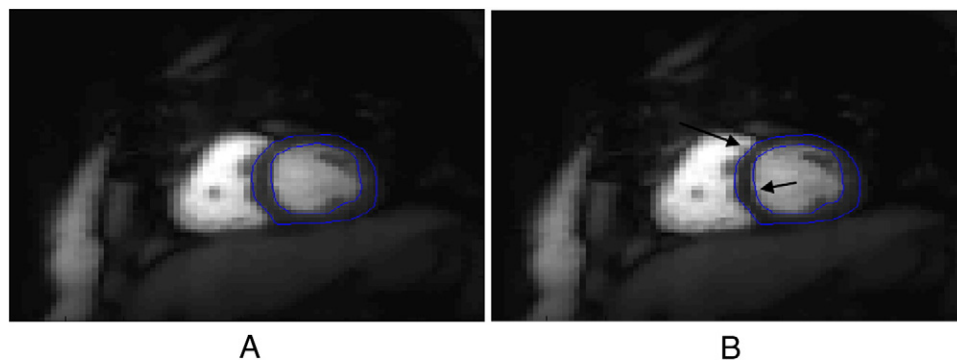
Fig. 8. The effect of EESTCR reconstructions on image segmentation is shown. The contours were drawn manually on STCR and overlaid on EESTCR. (A) Image reconstructed using STCR with its contour. (B) Image reconstructed using EESTCR with the contour from STCR overlaid on it. The contour from STCR is larger relative to EESTCR, and signal from the blood pool from LV and RV gets included with the myocardium. The regions where a more conservative contour would have been drawn in the EESTCR image are shown by the two arrows.

4.1. Loss of contrast due to TV minimization

TV minimization assumes that images are piecewise smooth or piecewise constant. This is often not true for medical images. Exact solutions for the change in intensity that is caused by TV were derived by Strong and Chan for simple images that have step edges like circles and rectangles and linearly varying edges [19,20,22]. It was shown that this change can be an increase or decrease of the original intensity and usually will be a direction that causes a decrease in contrast in the region. On a step edge, TV will cause the intensity of the lower edge to increase and the intensity of the higher edge to decrease, causing a decrease in contrast. With EESTCR, these increases of intensity at the lower edge and decrease of intensity at the higher edge have been avoided. In the difference image, the myocardial regions show negative intensity values, and the edges towards the LV and RV show positive values as shown in Figs. 3(D) and 4(D). The direction in which EESTCR causes a change in intensity at the edges matches the theoretical results predicted in Refs. [19,20,22].

4.2. Reference image and computational complexity

The reference images required for the spatially varying edge maps are extracted from the undersampled k-space data by combining multiple time frames in a sliding window fashion. As separate training data are not required to form the reference image, there is no additional acquisition time. Also, the formation of the reference image and the extraction of an edge map are computationally inexpensive. This edge map is similar to the one defined by Perona and Malik in Ref. [26] for denoising using anisotropic diffusion. But in anisotropic diffusion, a reference image-based method was not used for denoising the images.

The coils were reconstructed independently and then combined using the square root of sum of squares method. This helped reduce the reconstruction time by using the parallel processing toolbox in MATLAB to reconstruct the coils in parallel. On a Linux machine with 8 GB RAM and four

processors, reconstruction of one slice with 66 time frames took 413 s and 457 s with STCR and EESTCR, respectively.

5. Conclusion

EESTCR is a promising technique to reconstruct DCE cardiac perfusion images from undersampled k-space data. The resulting images have sharper edges and higher contrast when compared to STCR. The method is robust to some motion. The method is also applicable to other DCE imaging techniques such as DCE tumor imaging of the brain or breast, where motion-related problems are less than with cardiac imaging. Small features like edges in the myocardium were better reconstructed in EESTCR, and there was improvement in contrast. Improvement in CNR and contrast was seen in the LV blood pool–myocardium region. The mean improvement was 36% for CNR and 24% for contrast compared to a similar method without use of the edge information.

References

[1] Donoho DL. Compressed sensing. IEEE Trans Inf Theory 2006;52: 1289.

[2] Hu X. On the "keyhole" technique. J Magn Reson Imaging 1994;4:231.

[3] van Vaals JJ, Brummer ME, Dixon WT, Tuithof HH, Engels H, Nelson RC, et al. "Keyhole" method for accelerating imaging of contrast agent uptake. J Magn Reson Imaging 1993;3:671.

[4] Chandra S, Liang ZP, Webb A, Lee H, Morris HD, Lauterbur PC. Application of reduced-encoding imaging with generalized-series reconstruction (RIGR) in dynamic MR imaging. J Magn Reson Imaging 1996;6:783.

[5] Webb AG, Liang ZP, Magin RL, Lauterbur PC. Applications of reduced-encoding MR imaging with generalized-series reconstruction (RIGR). J Magn Reson Imaging 1993;3:925.

[6] Markl M, Hennig J. Phase contrast MRI with improved temporal resolution by view sharing: k-space related velocity mapping properties. Magn Reson Imaging 2001;19:669.

[7] Tsao J, Boesiger P, Pruessmann KP. k-t BLAST and k-t SENSE: dynamic MRI with high frame rate exploiting spatiotemporal correlations. Magn Reson Med 2003;50:1031.

[8] Otazo R, Kim D, Axel L, Sodickson DK. Combination of compressed sensing and parallel imaging for highly accelerated first-pass cardiac perfusion MRI. Magn Reson Med 2010;64:767.

[9] Xu D, King KF, Liang ZP. Improving k-t SENSE by adaptive regularization. Magn Reson Med 2007;57:918.

[10] Jung H, Park J, Yoo J, Ye JC. Radial k-t FOCUSS for high-resolution cardiac cine MRI. Magn Reson Med 2010;63:68.

[11] Jung H, Sung K, Nayak KS, Kim EY, Ye JC. k-t FOCUSS: a general compressed sensing framework for high resolution dynamic MRI. Magn Reson Med 2009;61:103.

[12] Lustig M, Santos JM, Donoho DL, Pauly JM. k-t SPARSE: High frame rate dynamic MRI exploiting spatio-temporal sparsity. In: Proceedings of the 13th Annual Meeting of ISMRM, Seattle, 2006. p. 2420.

[13] Ji JX, Zhao C, Lang T. Compressed sensing parallel magnetic resonance imaging. Conf Proc IEEE Eng Med Biol Soc 2008;2008:1671.

[14] Liang D, Liu B, Wang J, Ying L. Accelerating SENSE using compressed sensing. Magn Reson Med 2009;62:1574.

[15] Adluru G, Awate SP, Tasdizen T, Whitaker RT, DiBella EV. Temporally constrained reconstruction of dynamic cardiac perfusion MRI. Magn Reson Med 2007;57:1027.

[16] Adluru G, McGann C, Speier P, Kholmovski EG, Shaaban A, DiBella EV. Acquisition and reconstruction of undersampled radial data for myocardial perfusion magnetic resonance imaging. J Magn Reson Imaging 2009;29:466.

[17] Adluru G, Whitaker RT, DiBella EVR. Spatio-temporal constrained reconstruction of sparse dynamic contrast enhanced radial MRI data.

Proc 4th IEEE International Symposium on Biomedical Imaging (ISBI); 2007.

[18] Huang F, Chen Y, Yin W, Lin W, Ye X, Guo W, et al. A rapid and robust numerical algorithm for sensitivity encoding with sparsity constraints: self-feeding sparse SENSE. Magn Reson Med 2010;64: 1078.

[19] Strong D, Chan T. Edge and scale-dependent properties of total variation regularization. Inverse Problems 2003:19.

[20] Strong D, Chan T. Spatially and scale adaptive total variation based regularization and anisotropic diffusion in image processing. Diffusion in Image Processing, UCLA Math Department CAM Report; 1996.

[21] Kamesh Iyer S, DiBella EVR, Tasdizen T. Edge enhanced spatio-temporal constrained reconstruction of undersampled dynamic contrast enhanced radial MRI. Proc ISBI 2010:704.

[22] Strong D, Chan T. Exact solutions to total variation regularization problems. UCLA CAM Report; 1996.

[23] Candes E, Romberg J, Tao T. Robust uncertainty principles: exact signal reconstruction from highly incomplete frequency information. IEEE Trans Inf Theory 2006.

[24] Rudin LI, Osher S, Fatemi E. Nonlinear total variation based noise removal algorithms. Physica 1992;60:259.

[25] Karniadakis GEM, Kirby RM. Parallel scientific computing in C++ and MPI. New York: Cambridge University Press; 2003.

[26] Perona P, Malik J. Scale-space and edge detection using anisotropic diffusion. IEEE Trans Pattern Anal Mach Intell 1990;12:629.